NMR Spectroscopy

Local Structure and Anisotropic Backbone Dynamics from Cross-Correlated NMR Relaxation in Proteins**

Phineus R. L. Markwick, Remco Sprangers, and Michael Sattler**

The molecular function of biomacromolecules is determined by both their 3D structure and conformational dynamics. NMR cross-correlated relaxation (CCR) contains information about local structure and local anisotropic dynamics. CCR arises from the interference of two relaxation mechanisms such as chemical shift anisotropy (CSA) and dipole–dipole (DD) interactions, which are described by tensors in 3D space, and contains information about the relative orientation of these tensors and their correlated motion.[1–4] In this respect, CCR rates involving CSA tensors are most useful, as they sample local structure and dynamics along three orthogonal axes. Over the past few years, numerous NMR experiments have been designed to measure cross-correlated relaxation rates to determine local molecular geometry,[3,5] to study local dynamics,[6–9] and to characterize chemical-shift tensors in solution.[10–12] Different models of anisotropic local motion of the peptide plane have been discussed.[7,9,13–15]

Whereas CCR processes in principle contain an enormous amount of information, the interpretation of these relaxation rates must be treated with great care. For example, a CSA/DD relaxation process depends on many factors, including the local molecular structure, the magnitude of the CSA and orientation of the shift tensor in the fixed molecular frame, and local anisotropic dynamics.[2] To simplify this problem, the magnitude of the CSA and orientation of the shift tensor, both of which are difficult to access experimentally and theoretically, are often treated as fixed invariable parameters. Alternatively, the effect of dynamics is included through a generalized (isotropic) order parameter, which represents a considerable simplification to the complex hierarchy of internal anisotropic dynamic modes that characterize the local motion of the peptide plane. Recently, the vector fluctuations of N–H and $C'–C^{\alpha}$ bonds were monitored by studying the temperature dependence of cross-correlated relaxation rates rather than their absolute values, thereby diminishing the influence of uncertainties in CSA parameters.[9]

[*] Dr. P. R. L. Markwick, Dr. R. Sprangers, Dr. M. Sattler
European Molecular Biology Laboratory (EMBL)
Meyerhofstrasse 1, 69117 Heidelberg (Germany)
Fax: (+49) 6221-387-306
E-mail: markwick@embl.de
sattler@embl.de

[**] We thank Dr. M. Nilges, Professor R. Brüschweiler, Dr. B. Simon and C. Roome for discussions, P.R.L.M. acknowledges an EMBO fellowship. This work was supported by the DFG and the EU (D-LAB).

Supporting information for this article is available on the WWW under http://www.angewandte.org or from the author.

  DOI: 10.1002/ange.200462495

With extended DFT calculations, we previously found significant site-specific variations in both the magnitude of the C′ CSA (the relative magnitudes of the three principal components of the shift tensor δ_{11}, δ_{22}, and δ_{33}) and the orientation of the C′ chemical-shift tensor (with principal axes ξ_{11}, ξ_{22}, and ξ_{33}; Figure 1). We formulated a simple model for the C′ CSA, which depends only on the isotropic chemical shift, δ_{iso}.[16] The δ_{11} and δ_{33} components are ostensibly

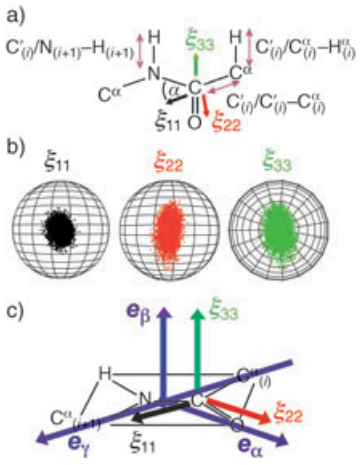

Figure 1. a) Schematic representation of the three C′ CSA/DD CCR rates studied. The average orientation of the C′ chemical-shift tensor (angle α) is also indicated (principal axes ξ_{11}, ξ_{22}, and ξ_{33}). The ξ_{33} axis lies perpendicular to the peptide plane, whereas the ξ_{11} and ξ_{22} axes lie in the peptide plane. b) Temporal fluctuations of the peptide plane of Val126 over the MD simulation. c) Representation of the average orientation of the C′ chemical-shift tensor (principal axes ξ_{11}, ξ_{22}, and ξ_{33}) and average GAF principal axes ($\boldsymbol{e}_\alpha$, $\boldsymbol{e}_\beta$, and $\boldsymbol{e}_\gamma$) in the local molecular frame.

invariable with average values of 247 ± 2 ppm and 85 ± 1 ppm, whereas the δ_{22} component varies linearly with the isotropic chemical shift ($\delta_{22} = 3\delta_{iso} - 332$ ppm). The parameterization of our CSA model[16] is notably improved in comparison with previous proposals,[17,18] and is supported by a recent analysis of experimental CCR rates, although local anisotropic motion was not explicitly considered in this study.[12] We also found that the orientation of the shift tensor is site-specific with the average α angle (the angle between ξ_{11} and the C′–N bond; Figure 1) varying from 22°–46°.[16]

Herein we combine classical molecular dynamics (MD) and extended DFT simulation methods with multidimensional NMR spectroscopy to study transverse C′ CSA/DD CCR processes. The extended DFT calculations provide an accurate representation of the C′ CSA magnitude and the orientation of the chemical-shift tensor in the fixed molecular frame. The MD simulation contains information about local anisotropic dynamics. Thus, by combining DFT and MD we can consider the relevant factors that affect the CCR rates and dissect their relative contributions.[2] Employing the Gaussian Axial Fluctuation (GAF) model,[19,20] we study local anisotropic fluctuations of the peptide plane orientation and provide an efficient method to determine these from cross-correlated relaxation.

We have measured three CSA/DD cross-correlated relaxation rates involving the carbonyl CSA: $C'_{(i)}/C^{\alpha}_{(i)}-H^{\alpha}_{(i)}$, $C'_{(i)}/N_{(i+1)}-H_{(i+1)}$, and $C'_{(i)}/C'_{(i)}-C^{\alpha}_{(i)}$ (Figure 1) for the 55-residue Tudor domain. A CSA/DD CCR rate, $\Gamma^{(CSA/DD)}$, associated with the interference of a chemical-shift tensor centered at nucleus J and a magnetic dipole–dipole interaction between nuclei K and L is given by:[1,3,4]

$$\Gamma^{(CSA/DD)}{}_{J/K-L} = 2\,d\,c \sum_i \{\delta_{ii}\, 4J^{cc}_{ii,K-L}(0)\} \tag{1}$$

in which $d = \sqrt{(1/8)}\,(\mu_0/4\pi)\,(h/2\pi)\,\gamma_K\,\gamma_L\,\langle r^{-3}_{K-L}\rangle$ and $c = \sqrt{(1/8)}\,\gamma_J B_0$ are constant factors for the dipolar and CSA interactions, respectively (Supporting Information).[*]

The cross-correlated spectral density functions, $J^{cc}_{ii,K-L}(\omega)$, are associated with the average relative orientation and temporal correlated motion between the i^{th} principal axis of the chemical-shift tensor and the K–L dipolar interaction. Assuming time-scale separation for slow isotropic rotation diffusion with an associated correlation time, τ_c, and fast local anisotropic motion, the spectral density function can be obtained by Fourier transformation of the associated cross-correlation function as:[1,3,4]

$$J^{cc}_{ii,K-L}(\omega) = 2\int_0^{\infty} C_{ii,K-L}(t)\,cos\,\omega t\,dt \tag{2a}$$

$$C_{ii,K-L}(t) = 1/5^{(t/\tau_c)}\,C^{int}_{ii,K-L}(t) \tag{2b}$$

$$C^{int}_{ii,K-L}(t) = \langle \boldsymbol{d}_{K-L}(0)\,\xi_{ii}(t)\rangle \equiv \langle P_2\,(cos\,\theta_{ii,K-L}(t))\rangle \tag{2c}$$

The first and second terms on the right side of Equation (2b) describe the correlation functions for internal motion assuming overall isotropic tumbling, which is a reasonable assumption for the Tudor domain (the ratio of $D_{\parallel}/D_{\perp} = 1.02$). The description of anisotropic rotational diffusion involves rather complex spectral densities,[3,21] and under certain limits the influence of anisotropic rotational diffusion can be approximated.[21] The values $\boldsymbol{d}_{K-L}$ and ξ_{ii} represent the orientation of the dipole–dipole interaction (K–L) and the principal chemical-shift tensor axes, respectively. $\theta_{ii,K-L}$ is the projection angle between the dipole–dipole vector and the i^{th} principal axis of the chemical-shift tensor. Herein, the spectral density functions in Equation (1) are derived numerically from the MD simulation according to Equation (2).

The cross-correlation functions can be expressed analytically with the model-free approach,[22,23] in which the average relative orientation and amplitude of the correlated motion of the two interaction vectors is defined by a single parameter, $S^2_{ii,K-L}$, known as the order parameter (Supporting Information). In the 3D GAF model, the anisotropic order parameter $S^2_{ii,K-L}$ is described by assuming Gaussian fluctuations around three principal axes, which are rigidly attached to the peptide plane. The 3D GAF parameters for the Tudor domain (principal axes $\boldsymbol{e}_\alpha$, $\boldsymbol{e}_\beta$, and $\boldsymbol{e}_\gamma$) and the standard deviation of

[*] Note that if K = J, that is, for a CCR that involves the CSA of spin J and a dipole–dipole interaction between spins J and L, $\Gamma^{(CSA/DD)}_{J,J-L} = 2\,d\,c \sum_i \{\delta_{ii}\,(4J^{cc}_{ii,J-L}(0) + 3J^{cc}_{ii,J-L}(\omega_J)\}$.

the angular fluctuations (σ_α, σ_β, σ_γ) have been extracted from a MD trajectory.[19,20]

Figure 2a shows the correlation between the simulated [Eq. (1) and Eq. (2)] and experimental C′/C$^\alpha$–H$^\alpha$ cross-correlated relaxation rates. In general, an excellent agreement between the experimental and simulated data is observed. Deviations are found for residues in loop regions, which, apart from Asp96, exhibit a low heteronuclear {^{1}H}–^{15}N NOE (<0.65). Presumably, these differences between simulation and experiment arise from incomplete sampling of ψ angles averaged over the MD simulation. Particularly in secondary structure elements, the motion of the C′ chemical-shift tensor principal axes and the C$^\alpha$–H$^\alpha$ bond vector is highly correlated, and the associated cross-correlation functions extracted from the MD trajectory exhibit almost no decay.

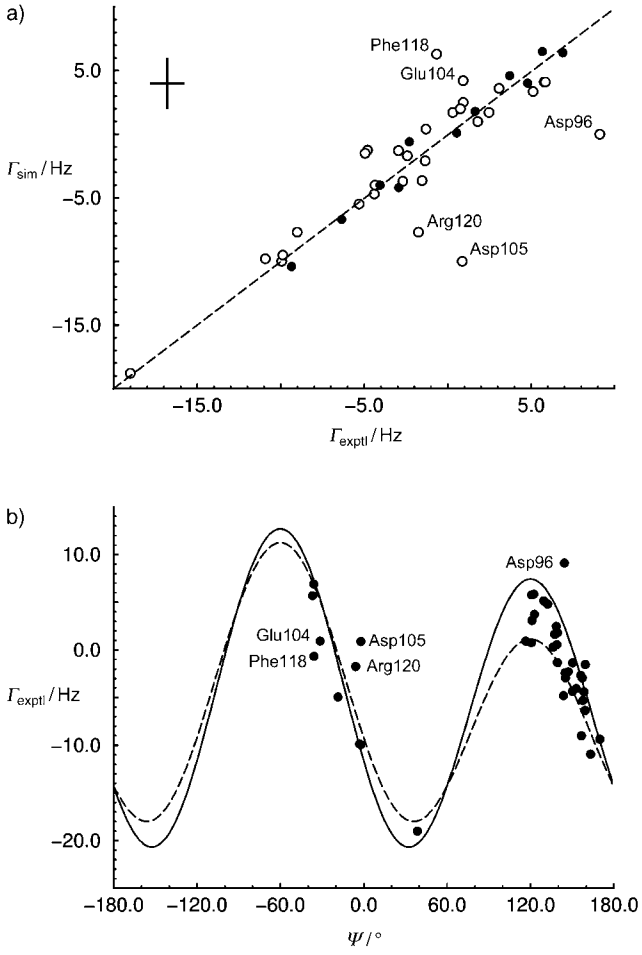

Figure 2. a) Experimental and simulated C′/C$^\alpha$–H$^\alpha$ CCR rates (Γ) for all residues in the Tudor domain excluding terminal residues and glycine residues. Filled and empty circles represent residues whose chemical-shift tensors were calculated with the extended DFT method or with the C′ CSA model, respectively. Under the model, the orientation of the shift tensor was fixed with $\alpha = 34°$. For five residues (labeled) the correlation between experiment and theory is poor. Each of these residues is in a loop region and, except for Asp96, exhibits a low heteronuclear {^{1}H}–^{15}N NOE (<0.65). b) Experimental C′/C$^\alpha$–H$^\alpha$ CCR rates plotted with respect to the ψ angle taken from the X-ray crystallographic structure.[34] Lines indicate the expected CCR rates assuming an C′ isotropic chemical shift of 168 ppm (-----) and 180 ppm (——). In both cases the orientation of the C′-shift tensor is fixed with $\alpha = 34°$.

This CCR process is predominantly dependent on the ψ angle, which determines the average orientation between the principal axes of the C′ shift tensor and the C$^\alpha$–H$^\alpha$ bond vector.[24–27] However, as can be observed in Figure 2b, site-specific variations of the C′ chemical-shift tensor also have an effect on the resulting relaxation rates, particularly when $60° < \psi < 180°$ for residues in β sheet secondary structure elements. Considering all residues studied in the Tudor domain, observed CCR rates vary between $-19.0\ s^{-1}$ and $+9.0\ s^{-1}$. The effect of C′ CSA variations causes a change in the relaxation rate of up to $7\ s^{-1}$ (25% of the total observed range), whereas the effect of dynamics (in secondary structure elements) only produces a change in the CCR rate of up to $2\ s^{-1}$ (7% variation). The orientation of the C′ chemical-shift tensor relative to the peptide plane has a small effect on the relaxation rate ($<3\ s^{-1}$) and is observed only in α-helical regions (Supporting Information).

This analysis indicates that when C′/C$^\alpha$–H$^\alpha$ CSA/DD CCR rates are used for refining the backbone angle ψ in secondary structure elements,[27,28] local dynamics has only a small effect on the measured rates. However, site-specific variations of the C′ CSA should clearly be taken into account. This can be addressed easily with the CSA model based on the isotropic C′ chemical shift.[16]

The C′/N–H CCR process depends predominantly on the C′ CSA (the magnitude of the δ_{22} component) and local anisotropic dynamics. This is highlighted in Figure 3, in which experimental and simulated CCR rates are compared with a fixed shift tensor[29] (Figure 3a) and our site-specific shift tensor[16] (Figure 3b); each case presents the simulated results with and without the inclusion of dynamics. On average, the ω angle is $180° \pm 5°$ in all residues studied, and such small variations in this angle have a negligible effect on the relaxation rates. Similarly, variations in the orientation of the C′-shift tensor in the fixed molecular frame (the α angle) have a very small effect on this CCR process (Supporting

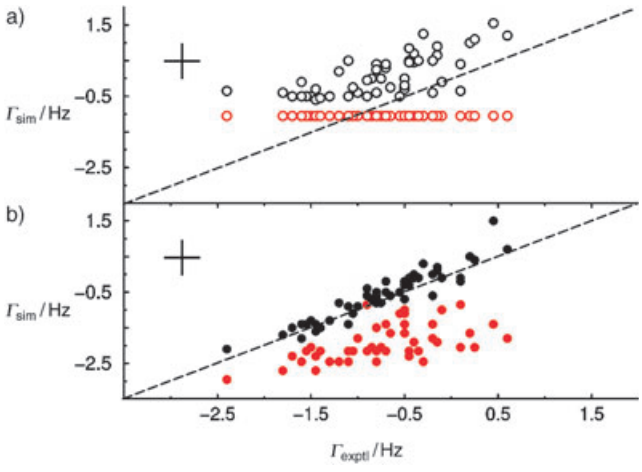

Figure 3. a) Experimental and simulated C′/N–H CCR rates assuming a fixed invariant C′ CSA[29] excluding (red ○) and including (black ○) the effect of local anisotropic dynamics. b) Experimental and simulated C′/N–H CCR rates with the site-specific C′-shift tensor excluding (red ●) and including (black ●) the effect of local anisotropic dynamics. In all cases a N–H bond length of 1.02 Å is employed, and the orientation of the C′ chemical-shift tensor is fixed with $\alpha = 34°$.

Information). This relaxation rate has been used previously to characterize local anisotropic dynamics—that of the peptide plane.[8,30] The analysis presented herein strongly argues that site-specific CSA variations have to be considered before extracting dynamic parameters from this CCR rate, as discussed below.

Experimental and simulated C′/C′–C^{α} cross-correlated relaxation rates for the 12 carbonyl groups studied with our extended DFT procedure are shown in Figure 4. This CCR

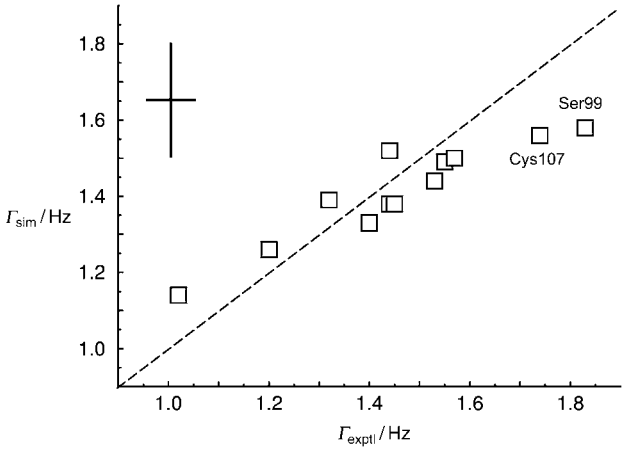

Figure 4. Correlation between experimental and simulated C′/C′–C^{α} CCR rates for the 12 residues studied with the extended DFT chemical-shift calculation.[16] The C′/C′–C^{α} CCR rate depends strongly on the orientation of the chemical-shift tensor (the α angle). Large CCR rates such as those of Ser99 and Cys107 are observed when the α angle is very large (> 42°). Unfortunately, it is difficult to accurately estimate the magnitude of the site-specific α angle. The α angle of each residue is therefore obtained directly from the DFT calculations.

process depends primarily on the orientation of the shift tensor in the molecular frame. A change in the α angle alone (Figure 1) from 20° to 50° causes a change in the C′/C′–C^{α} CCR rate of 0.6 s^{-1}, which covers the range of relaxation rates measured. Local anisotropic dynamics leads to variations that change the relaxation rate by up to 0.30 s^{-1} (50% of the total observed range). The variation in the carbonyl CSA can cause a change in the relaxation rate of up to 0.15 s^{-1} (25% of the total range). Therefore, local anisotropic dynamics contributes only partially to the observed variations in this CCR rate, and variations in the α angle have to be considered.

For C′/N–H and C′/C′–C^{α} CCR processes, local anisotropic motion of the peptide plane has a considerable effect on the observed relaxation rates. To further investigate the effect of local anisotropic motion on these CCR processes, we employed the 3D GAF model of Brüschweiler and coworkers.[20] This model is particularly useful, as it describes the motion of the peptide plane in terms of physically meaningful geometrical parameters. For all residues in the Tudor domain we found that the principal axis $\boldsymbol{e}_{\beta}$ sits perpendicular to the peptide plane and the $\boldsymbol{e}_{\gamma}$ axis lies at an angle of 36°–40° relative to the C′–N bond. The 3D GAF principal axes of rotation are therefore almost exactly co-oriented with the average DFT calculated principal axes of the C′-shift tensor in the fixed peptide frame (Figure 1). The standard deviations of amplitude fluctuations (σ_{α}, σ_{β}) over the MD trajectory of 10 ns change very little from residue to residue, with average values in the β-sheet regions (6 ± 2°, 4.5 ± 2°), in the 3_{10} helix (5 ± 2°, 4 ± 2°) and in the loop regions (11° ± 3°, 8° ± 3°). A significantly larger variation was observed in the fluctuation of σ_{γ} from 9° to 17° in the secondary structure elements and up to 25° in the more flexible loop regions. These results are similar to a previous analysis of ubiquitin based on a set of autocorrelated relaxation rates.[15]

Through simplification of the 3D GAF model to an effective 1D GAF model, in which $\sigma_{\alpha} = \sigma_{\beta} = 5° \equiv \sigma_{\alpha\beta}$ (the global average value for all residues in secondary structure elements) and by using the average orientation of the 3D GAF principal rotation axes, we have calculated the effect of the variation of σ_{γ} on the C′/N–H CCR rate. The resulting 2D CCR map (Figure 5), which includes the effect of site-specific

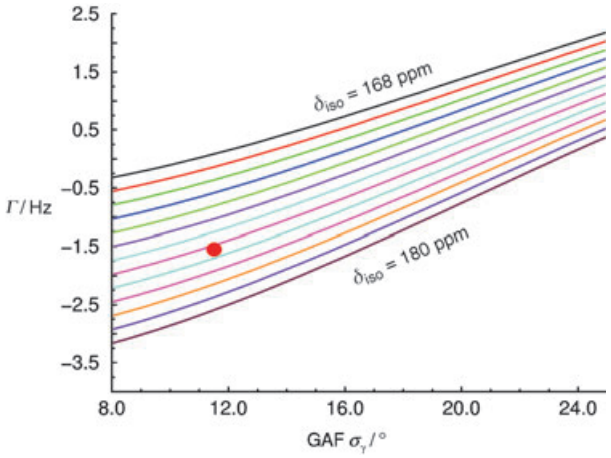

Figure 5. A 2D CCR map for C′/N–H CCR. From top to bottom, the isotropic C′ chemical shift varies from 168 to 180 ppm with lines drawn every 1 ppm; $\sigma_{\alpha\beta}$ is fixed at 5°. For a given C′/N–H CCR rate, the corresponding σ_{γ} can be extracted from the 2D map, as shown for Val126 (δ_{iso} = 175.3 ppm; C′/N–H CCR rate = −1.6 Hz).

C′ CSA variations, allows the accurate estimation of σ_{γ} from a given experimental C′/N–H CCR rate. As shown in detail in the Supporting Information, variations in the orientation of the C′-shift tensor and $\sigma_{\alpha\beta}$ generally have a negligible effect on this CCR process. The resulting σ_{γ} amplitude fluctuations correlate very well with the autocorrelated ^{15}N order parameter calculated from ^{15}N relaxation data with TENSOR2[31] (Figure 6). This important result demonstrates that the different relaxation rates provide a consistent description of the local anisotropic dynamics. This observation also argues that out-of-plane motion of the N–H bond vector[9,32] does not have a strong effect on these relaxation rates.[*] Given the larger amplitude of σ_{γ} compared with $\sigma_{\alpha\beta}$, our GAF analysis is

[*] In fact, this is indicated by comparing C′/N–H cross-correlated order parameters calculated numerically from the MD simulation [Eq. (1) and Eq. (2)] with the order parameters extracted from the 3D GAF analysis of the same simulation. The difference in the numerically calculated order parameters (which include N–H out-of-plane motion) and the 3D GAF order parameters (which do not sense N–H out-of-plane motion) is less than 0.03, resulting in a negligible change in the associated CCR rates.

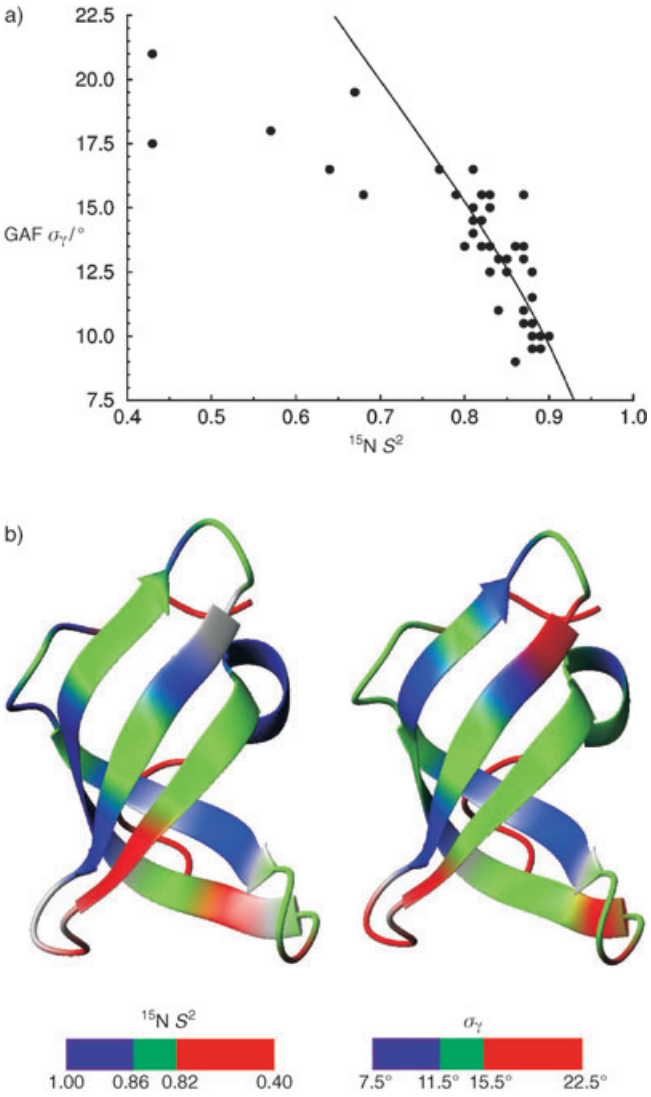

Figure 6. a) Correlation between the order parameter S^2 extracted from ^{15}N autorelaxation rates and σ_γ, which is extracted from the analysis of C′/N–H cross-correlated relaxation data. Assuming that $\sigma_\alpha = \sigma_\beta = 5°$, the theoretically expected correlation[19,20] is indicated by the solid line. For residues in secondary structure elements with the ^{15}N order parameter $S^2 = 0.75$, the result is in good agreement with the expected correlation. For the more flexible residues in terminal loop regions, a distinct deviation is observed. This results partly from the fact that for these residues, $\sigma_{\alpha\beta}$ is much larger than 5°, and also from the fact that for these very flexible regions, the 3D GAF model breaks down. b) Representation of the variations of the ^{15}N order parameter S^2 and σ_γ visualized on the Tudor domain. Residues for which no experimental data are available are rendered in gray.

consistent with so-called crankshaft motions around the $C^\alpha_{(i)} \cdots C^\alpha_{(i+1)}$ axis (Figure 1c).[7,13–15] We have also calculated 2D CCR maps for the C′/C′–C$^\alpha$ CCR rate, which demonstrate the strong dependence of this rate on the orientation of the C′-shift tensor and variations in $\sigma_{\alpha\beta}$ (Supporting Information).

In summary, we have performed a detailed analysis of C′ CSA/DD CCR rates by combining classical MD and extended DFT simulation methods. We have found that the C′/C$^\alpha$–H$^\alpha$ CCR rate depends primarily on the local protein structure (the ψ angle), but is also affected by variations in the C′ CSA. In contrast, the C′/C′–C$^\alpha$ CCR rate strongly depends on the orientation of the carbonyl chemical-shift tensor in the fixed molecular frame and local anisotropic dynamics, but C′ CSA variations also play a role. The C′/N–H CCR rate depends principally on the carbonyl CSA (the magnitude of δ_{22}) and local anisotropic dynamics and is thus most useful for the characterization of such motions. Employing the 3D GAF model, it is possible to acquire detailed information concerning the local anisotropic motion of the peptide plane from a single cross-correlation: the C′/N–H CCR rate.

Cross-correlated relaxation processes contain a wealth of information concerning both the structure and dynamics of biomolecular systems and are exploited in the design of relaxation-optimized NMR experiments.[33] The improved description of the parameters presented herein will be useful for future studies of the characterization of local anisotropic dynamics. A dissection of the relaxation data into different contributing factors demonstrates the power of combining theoretical and experimental techniques to probe the structure and dynamics of biomacromolecules.

Received: November 2, 2004
Revised: January 10, 2005
Published online: April 21, 2005

Keywords: chemical shift anisotropy · density functional calculations · molecular dynamics · NMR spectroscopy · structure elucidation

[1] M. W. F. Fischer, A. Majumdar, E. R. P. Zuiderweg, *Prog. Nucl. Magn. Reson. Spectrosc.* **1998**, *33*, 207.
[2] C. Scheurer, N. R. Skrynnikov, S. F. Lienin, S. K. Straus, R. Brüschweiler, R. R. Ernst, *J. Am. Chem. Soc.* **1999**, *121*, 4242.
[3] H. Schwalbe, T. Carlomagno, M. Hennig, J. Junker, B. Reif, C. Richter, C. Griesinger, *Methods Enzymol.* **2001**, *338*, 35.
[4] D. Frueh, *Prog. Nucl. Magn. Reson. Spectrosc.* **2002**, *41*, 305.
[5] B. Reif, M. Hennig, C. Griesinger, *Science* **1997**, *276*, 1230.
[6] M. W. F. Fischer, L. Zeng, Y. X. Pang, W. D. Hu, A. Majumdar, E. R. P. Zuiderweg, *J. Am. Chem. Soc.* **1997**, *119*, 12629.
[7] M. W. F. Fischer, L. Zeng, A. Majumdar, E. R. P. Zuiderweg, *Proc. Natl. Acad. Sci. USA* **1998**, *95*, 8016.
[8] T. Carlomagno, M. Maurer, M. Hennig, C. Griesinger, *J. Am. Chem. Soc.* **2000**, *122*, 5105.
[9] T. Wang, S. Cai, E. R. P. Zuiderweg, *J. Am. Chem. Soc.* **2003**, *125*, 8639.
[10] Y. Pang, E. R. P. Zuiderweg, *J. Am. Chem. Soc.* **2000**, *122*, 4841
[11] D. Fushman, D. Cowburn, *Methods Enzymol.* **2001**, *339*, 109.
[12] F. Cisnetti, K. Loth, P. Pelupessy, G. Bodenhausen, *ChemPhysChem* **2004**, *5*, 807.
[13] A. R. Fadel, D. Q. Jin, G. T. Montelione, R. M. Levy, *J. Biomol. NMR* **1995**, *6*, 221.
[14] R. M. Levy, M. Karplus, *Biopolymers* **1979**, *18*, 2465.
[15] S. F. Lienin, T. Bremi, B. Brutscher, R. Brüschweiler, R. R. Ernst, *J. Am. Chem. Soc.* **1998**, *120*, 9870.
[16] P. R. L. Markwick, M. Sattler, *J. Am. Chem. Soc.* **2004**, *126*, 11424.
[17] T. G. Oas, C. Y. Hartzell, T. J. McMahon, G. P. Drobny, F. W. Dahlquist, *J. Am. Chem. Soc.* **1987**, *109*, 5956.
[18] N. Asakawa, S. Kuroki, H. Kurosu, I. Ando, A. Shoji, T. Ozaki, *J. Am. Chem. Soc.* **1992**, *114*, 3261.
[19] R. Brüschweiler, P. E. Wright, *J. Am. Chem. Soc.* **1994**, *116*, 8426.
[20] T. Bremi, R. Brüschweiler, *J. Am. Chem. Soc.* **1997**, *119*, 6672.

[21] M. Deschamps, *J. Phys. Chem. A* **2002**, *106*, 2438.
[22] G. Lipari, A. Szabo, *J. Am. Chem. Soc.* **1982**, *104*, 4546.
[23] G. Lipari, A. Szabo, *J. Am. Chem. Soc.* **1982**, *104*, 4559.
[24] D. Yang, R. Konrat, L. E. Kay, *J. Am. Chem. Soc.* **1997**, *119*, 11938.
[25] D. Yang, L. E. Kay, *J. Am. Chem. Soc.* **1998**, *120*, 9880.
[26] E. Chiarparin, P. Pelupessy, R. Ghose, G. Bodenhausen, *J. Am. Chem. Soc.* **1999**, *121*, 6876.
[27] R. Sprangers, M. J. Bottomley, J. P. Linge, J. Schultz, M. Nilges, M. Sattler, *J. Biomol. NMR* **2000**, *16*, 47.
[28] B. Reif, A. Diener, M. Hennig, M. Maurer, C. Griesinger, *J. Magn. Reson.* **2000**, *143*, 45.
[29] Q. Teng, M. Iqbal, T. A. Cross, *J. Am. Chem. Soc.* **1992**, *114*, 5312.
[30] B. Brutscher, N. R. Skrynnikov, T. Bremi, R. Brüschweiler, R. R. Ernst, *J. Magn. Reson.* **1998**, *130*, 346.
[31] P. Dosset, J. C. Hus, M. Blackledge, D. Marion, *J. Biomol. NMR* **2000**, *16*, 23.
[32] T. S. Ulmer, B. E. Ramirez, F. Delaglio, A. Bax, *J. Am. Chem. Soc.* **2003**, *125*, 9179.
[33] K. Pervushin, R. Riek, G. Wider, K. Wüthrich, *Proc. Natl. Acad. Sci. USA* **1997**, *94*, 12366.
[34] R. Sprangers, M. R. Groves, I. Sinning, M. Sattler, *J. Mol. Biol.* **2003**, *327*, 507.

